THE JOURNAL OF BIOLOGICAL CHEMISTRY VOL. 281, NO. 42, pp. 32015–32024, October 20, 2006

Allosteric Control of Cyclic di-GMP Signaling*[S]

Received for publication, April 13, 2006, and in revised form, June 21, 2006 Published, JBC Papers in Press, August 21, 2006, DOI 10.1074/jbc.M603589200

Beat Christen[‡1], Matthias Christen[‡1], Ralf Paul[‡], Franziska Schmid[§], Marc Folcher[‡], Paul Jenoe[‡], Markus Meuwly[§], and Urs Jenal[‡2]

From the [‡]Biozentrum and the [§]Department of Chemistry, University of Basel, Klingelbergstrasse 70, 4056 Basel, Switzerland

Cyclic di-guanosine monophosphate is a bacterial second messenger that has been implicated in biofilm formation, antibiotic resistance, and persistence of pathogenic bacteria in their animal host. Although the enzymes responsible for the regulation of cellular levels of c-di-GMP, diguanylate cyclases (DGC) and phosphodiesterases, have been identified recently, little information is available on the molecular mechanisms involved in controlling the activity of these key enzymes or on the specific interactions of c-di-GMP with effector proteins. By using a combination of genetic, biochemical, and modeling techniques we demonstrate that an allosteric binding site for c-di-GMP (I-site) is responsible for non-competitive product inhibition of DGCs. The I-site was mapped in both multi- and single domain DGC proteins and is fully contained within the GGDEF domain itself. *In vivo* selection experiments and kinetic analysis of the evolved I-site mutants led to the definition of an *RXXD* motif as the core c-di-GMP binding site. Based on these results and based on the observation that the I-site is conserved in a majority of known and potential DGC proteins, we propose that product inhibition of DGCs is of fundamental importance for c-di-GMP signaling and cellular homeostasis. The definition of the I-site binding pocket provides an entry point into unraveling the molecular mechanisms of ligand-protein interactions involved in c-di-GMP signaling and makes DGCs a valuable target for drug design to develop new strategies against biofilm-related diseases.

A global signaling network that relies on the production of the second messenger cyclic diguanylic acid has recently been discovered in bacteria (1, 2). The c-di-GMP[3] system emerges as a regulatory mastermind orchestrating multicellular behavior and biofilm formation in a wide variety of bacteria (2). In addition, c-di-GMP signaling also plays a role in bacterial virulence and persistence (3–7). The broad importance of this novel signaling molecule in pathogenic and non-pathogenic bacteria calls for careful analysis of the molecular mechanisms that control cellular levels of c-di-GMP and regulate its downstream targets. c-di-GMP is formed by the condensation of two GTP molecules (8–10) and is hydrolyzed to GMP via the linear intermediate pGpG (11–14). Two widespread and highly conserved bacterial protein domains have been implicated in the synthesis and hydrolysis of c-di-GMP, respectively (15). The breakdown of c-di-GMP is catalyzed by the EAL domain (12–14), and the diguanylate cyclase (8) activity resides in the GGDEF domain (10, 16). The highly conserved amino acid sequence GG(D/E)EF forms part of the catalytically active site (A-site) of the DGC enzyme (8). In agreement with this, mutations that change the GG(D/E)EF motif generally abolish the activity of the respective proteins (14, 16–18).

GGDEF domains are often found associated with sensor domains, arguing that DGC activity is controlled by direct signal input through these domains (1). The best understood example for controlled activation of a DGC is the response regulator PleD, which constitutes a timing device for *Caulobacter crescentus* pole development (17, 19, 20). PleD is activated during *C. crescentus* development by phosphorylation of an N-terminal receiver domain and, as a result, sequesters to the differentiating cell pole (17, 19). An additional layer of control was suggested by the crystal structure of PleD solved recently in complex with c-di-GMP (8) (Fig. 1). A c-di-GMP binding site was identified in the crystal, spatially separated from the catalytically active site (A-site). Two mutually intercalating c-di-GMP molecules were found tightly bound to this site, at the interface between the GGDEF and the central receiver-like domain of PleD (Fig. 1). Based on the observation that PleD activity shows a strong non-competitive product inhibition, it was proposed that this site might constitute an allosteric binding site (I-site) (8). Based on the observation that functionally important residues of the PleD I-site are highly conserved in a majority of GGDEF proteins listed in the data base, we tested the hypothesis that allosteric product inhibition is a general regulatory principle of bacterial diguanylate cyclases.

MATERIALS AND METHODS

Strains, Plasmids, and Media—Escherichia coli and *Salmonella enterica* serovar Typhimurium strains were grown in Luria broth (LB). *C. crescentus* strains were grown in complex peptone yeast extract (21). For DGC activity assays *in vivo*, *E. coli* was plated onto LB Congo Red plates (Sigma, 50 μg/ml). To determine the IPTG induction phenotype, 3 μl of a liquid log phase culture was spotted onto LB Congo Red plates with-

* This work was supported by Swiss National Science Foundation Fellowship 3100A0-108186 (to U. J.) and by a Swiss National Science Foundation Förderprofessur (to M. M.). The costs of publication of this article were defrayed in part by the payment of page charges. This article must therefore be hereby marked "*advertisement*" in accordance with 18 U.S.C. Section 1734 solely to indicate this fact.

[S] The on-line version of this article (available at http://www.jbc.org) contains supplemental text and Figs. S1–S4.

[1] These authors contributed equally to this work.

[2] To whom correspondence should be addressed: Tel.: 41-61-267-2135; Fax: 41-61-267-2118; E-mail: urs.jenal@unibas.ch.

[3] The abbreviations used are: c-di-GMP, cyclic diguanylic acid; pGpG, linear diguanylic acid; LB, Luria broth; DGC, diguanylate cyclase; PDE, phosphodiesterase; H6, hexa-histidine tag; rdar, red, dry, and rough; IPTG, isopropyl 1-thio-β-D-galactopyranoside; DgcA, diguanylate cyclase A; PdeA, phosphodiesterase A; CR, Congo Red; AC, adenylate cyclase; GC, guanylate cyclase.

out and with 1 mM IPTG. Biofilm formation was quantified after overnight growth by staining with 1% Crystal Violet as described (22). Motility phenotypes were determined using LB or peptone yeast extract motility plates containing 0.3% Difco-Agar. The exact procedure of strain and plasmid construction is available on request.

Random I-site Tetrapeptide Library—The *dgcA* gene (CC3285) was amplified by PCR using primers #1006 and #1007 (for primer list see supplemental text). The PCR product was digested with NdeI and XhoI and cloned into pET21a (Novagen). In a next step a *dgcA*ΔRESD allele with a silent PstI restriction site was generated by splicing with overlapping extension PCR using primers #1129, #670, and #1132. The resulting PCR product was digested with NdeI and XhoI and cloned into pET42b (Novagen) to produce pET42::dgcAΔRESD. The PstI/XhoI fragment of pET42b::dgcAΔRESD was replaced by 20 independent PCR products, which had been generated using pET42b::dgcAΔRESD as a template and primers #1131 and #670. The resulting 20 independent random libraries were individually transformed into *E. coli* BL21 and screened on Congo Red plates (LB plates supplemented with 50 μg/ml Congo Red). As a control reaction, the deleted I-site was reverted back to the wild-type RESD motif by cloning the PCR product generated with primers #1130 and #670 into the PstI and XhoI site of pET42b::dgcAΔRESD.

Diguanylate Cyclase and Phosphodiesterase Activity Assays—DGC reactions were performed at 30 °C with 0.5 μM purified hexahistidine-tagged DgcA or 5 μM PleD in DGC reaction buffer containing 250 mM NaCl, 25 mM Tris-Cl, pH 8.0, 5 mM β-mercaptoethanol, and 20 mM $MgCl_2$. For inhibition assays the protein was preincubated with different concentrations of c-di-GMP (1–100 μM) for 2 min at 30 °C before 100 μM [^{33}P]GTP (Amersham Biosciences) was added. The reaction was stopped at regular time intervals by adding an equal volume of 0.5 M EDTA, pH 8.0. DGC/PDE tandem assays were carried out using 1 μM hexahistidine-tagged DgcA, which was preincubated for 2 min in the presence or absence of 4.5 μM hexahistidine-tagged phosphodiesterase PdeA. The reaction was started by adding 100 μM [^{33}P]GTP. The reactions were stopped at regular time intervals of 15 s by adding equal volumes of 0.5 M EDTA, pH 8.0, and their nucleotide composition was analyzed as described below.

Initial velocity (V_o) and inhibition constants were determined by plotting the corresponding nucleotide concentration *versus* time and by fitting the curve according to allosteric product inhibited Michaelis-Menten kinetics with the program ProFit 5.6.7 (with fit function $[\text{c-di-GMP}]_t = a(1)^*t/(a(2) + t)$, where the initial velocity V_o is defined as $a(1)/a(2)$) using the Levenberg-Marquardt algorithm. K_i values were determined by plotting V_o *versus* c-di-GMP concentration and using the following fit function, $V_{o[\text{c-di-GMP}]} = V_{o[\text{c-di-GMP}]=0}{}^*(1 - ([\text{c-di-GMP}]/(K_i + [\text{c-di-GMP}]))$.

Polyethyleneimine Cellulose Chromatography—Samples were dissolved in 5 μl of running buffer containing 1:1.5 (v/v) saturated NH_4SO_4 and 1.5 M KH_2PO_4, pH 3.60, and blotted on Polygram® CEL 300 polyethyleneimine cellulose TLC plates (Macherey-Nagel). Plates were developed in 1:1.5 (v/v) saturated NH_4SO_4 and 1.5 M KH_2PO_4, pH 3.60 (R_f(c-di-GMP) 0.2, R_f(pGpG) 0.4), dried, and exposed on a storage phosphor imaging screen (Amersham Biosciences). The intensity of the various radioactive species was calculated by quantifying the intensities of the relevant spots using ImageJ software version 1.33. V_o and K_i were determined with the Software ProFit 5.6.7.

UV Cross-linking with [^{33}P]c-di-GMP—The ^{33}P-labeled c-di-GMP was produced enzymatically using [^{33}P]GTP (3000 Ci/mmol) and purified according to a previous study (14). Protein samples were incubated for 10 min on ice in DGC reaction buffer (25 mM Tris-HCl, pH 8.0, 250 mM NaCl, 10 mM $MgCl_2$, 5 mM β-mercaptoethanol) together with 1 μM c-di-GMP and ^{33}P-radiolabeled c-di-GMP (0.75 μCi, 6000 Ci/mmol). Samples were then irradiated at 254 nm for 20 min in an ice-cooled, parafilm-wrapped 96-well aluminum block in an RPR-100 photochemical reactor with a UV lamp RPR-3500 (Southern New England Ultraviolet Co.). After irradiation, samples were mixed with 2× SDS-PAGE sample buffer (250 mM Tris-HCl at pH 6.8, 40% glycerol, 8% SDS, 2.4 M β-mercaptoethanol, 0.06% bromphenol blue, 40 mM EDTA) and heated for 5 min at 95 °C. Labeled proteins were separated by SDS-PAGE and quantified by autoradiography.

Nucleotide Extraction and Analysis—2.0 ml of *E. coli* cell cultures (A_{600} 0.4) were harvested by centrifugation, and supernatant was discarded. The cell pellet was dissolved in 200 μl of 0.5 M formic acid, and nucleotides were extracted for 10 min at 4 °C. Insoluble cell components were then pelleted, and the supernatant was directly analyzed by chromatography. Nucleotides were extracted and separated according to a previous study (23) on a 125/4 Nucleosil 4000-1 polyethyleneimine column (Macherey-Nagel) using the SMART-System (Amersham Biosciences). The nucleotide peak corresponding to c-di-GMP was verified by co-elution with a chemically synthesized c-di-GMP standard.

DgcA Protein Expression Levels—DgcA protein expression levels in *E. coli* BL21 were determined by Western blot analysis using Anti-His(C-Term) antibody (Invitrogen) and horseradish peroxidase conjugate of goat anti-mouse IgG (Invitrogen) as secondary antibody. The protein concentration was determined by measuring the intensities of the relevant spots using ImageJ software version 1.33. Signals were calibrated to defined concentrations of purified wild-type DgcA.

Molecular Modeling of PleD—All-atom simulations were carried out using the CHARMM (24) program and the CHARMM22/27 force field (25). For additional information see the supplemental material.

RESULTS

Feedback Inhibition of the PleD Diguanylate Cyclase Requires Binding of c-di-GMP to the I-site—The PleD crystal structure indicated the existence of an allosteric binding pocket (I-site) at the interface of the GGDEF and REC2 domains (8). Binding of a c-di-GMP dimer in the I-site is mediated by specific electrostatic interactions with charged residues of the GGDEF and REC2 domain (Fig. 1). To provide evidence for c-di-GMP binding to the I-site pocket in solution, trypsin digests were performed with purified PleD protein (5 μM) in the presence or absence of c-di-GMP (25 μM). The resulting peptide fragments were separated on a C18 column and analyzed by matrix-as-

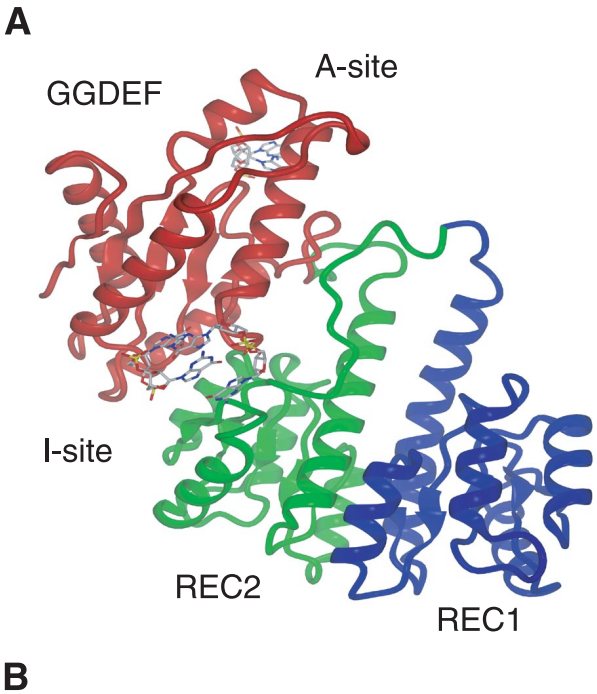

FIGURE 1. **Crystal structure of the response regulator PleD.** *A*, domain architecture of PleD with receiver domain REC1 (*blue*), receiver domain REC2 (*green*), and GGDEF domain harboring diguanylate cyclase activity (*red*). The active site (A-site) loop and the allosteric binding site (I-site) are indicated. *B*, zoom in view of the I-site pocket with a bound dimer of c-di-GMP with intercalated purine bases. Residues Arg-148 and Arg-178 (*green*) from the REC2 domain and residues Arg-359, Asp-362, and Arg-390 (*red*) from the GGDEF domain make specific contacts to the ligand in the crystal structure. *C*, schematic of c-di-GMP synthesis and degradation reactions.

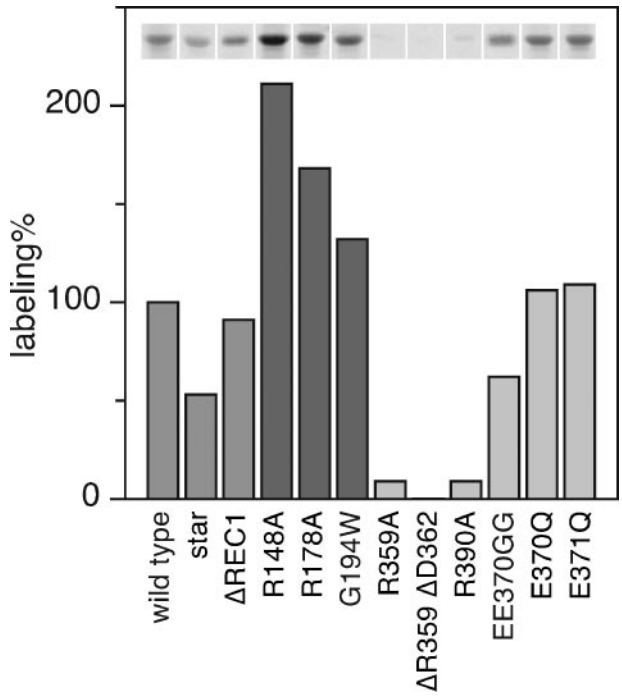

FIGURE 2. **c-di-GMP labeling efficiency of different PleD mutants.** The *upper lane* shows autoradiographs of [^{33}P]c-di-GMP UV cross-linked hexahistidine-tagged PleD mutant proteins separated by SDS-PAGE. Relative labeling efficiency with c-di-GMP is shown below with wild-type PleD corresponding to 100%. Specific mutants in different domains are colored in *gray* (REC1), *dark gray* (REC2) and *light gray* (GGDEF).

sisted laser desorption ionization time-of-flight. Both chromatograms were identical, with the exception of two peaks that were only detected in the absence of ligand but were protected when c-di-GMP present during tryptic digest (supplemental Fig. S1). One of the two peptides (T47, retention time 25.6 min) was identified by mass spectrometry and corresponds to the amino acids 354–359 (supplemental Fig. S1), arguing that c-di-GMP specifically protects from trypsin cleavage at Arg-359. To provide additional evidence for ligand binding in solution, we performed UV cross-linking assays using ^{33}P-labeled c-di-GMP (14). Residues Arg-148 and Arg-178 of the REC2 domain and Arg-359, Asp-362, and Arg-390 of the GGDEF domain were replaced with alanine, and the resulting protein variants were analyzed. As shown in Fig. 2, mutating I-site residues of the GGDEF domain abolished (ΔR359ΔD362) or strongly reduced (R359A and R390A) c-di-GMP binding. In contrast, mutations in the A-site (E370Q, E371Q, and EE370GG), which completely abolished enzymatic activity (Table 1), had no effect on c-di-GMP binding (Fig. 2), indicating that labeling with radioactive c-di-GMP results from ligand binding at the I-site. Although mutations R359A, R359V, ΔR359ΔD362, and D362A all showed a dramatically reduced or complete loss of enzymatic activity, mutant R390A showed wild-type-like DGC activity (Table 1). In agreement with the reduced binding of c-di-GMP (Fig. 2), the K_i of mutant R390A was increased ~20-fold (Table 1). PleD proteins harboring mutations in the REC2 portion of the I-site (R148A and R178A) showed an increased binding of c-di-GMP (Fig. 2) and slightly lower K_i values than wild type (Table 1). Surprisingly, R148A/R178A single and double mutants displayed a 5- to 20-fold higher DGC activity compared with wild-type PleD (Table 1). Finally, c-di-GMP binding was normal in mutant proteins that either lacked the REC1 receiver domain or had a bulky tryptophan residue introduced at the REC2-GGDEF interface (G194W, Fig. 2). Together these results implied that the structural requirements for c-di-GMP binding are contained within the GGDEF domain of PleD and that residues Arg-359, Asp-362, and Arg-390 form the core of an allosteric binding pocket for c-di-GMP.

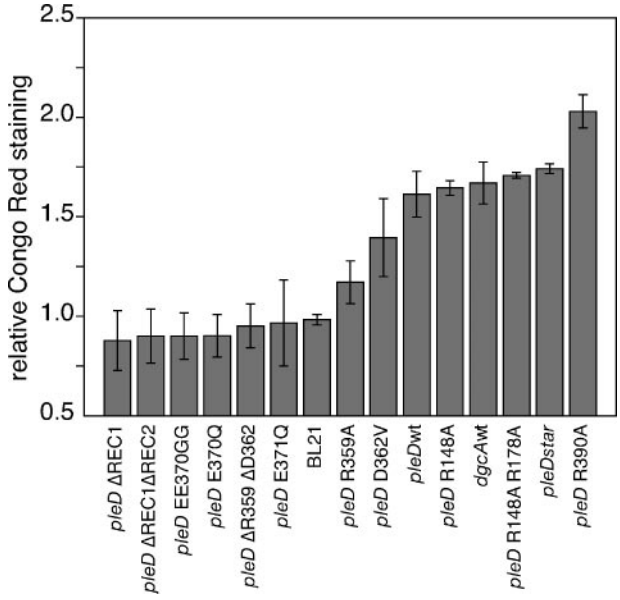

FIGURE 3. ***In vivo* activity of different PleD and DgcA mutant proteins.** *E. coli* BL21 strains expressing different *pleD* alleles and *dgcA* wild type were spotted onto Congo Red plates. Relative Congo Red binding was determined using imageJ software with BL21 corresponding to 100%.

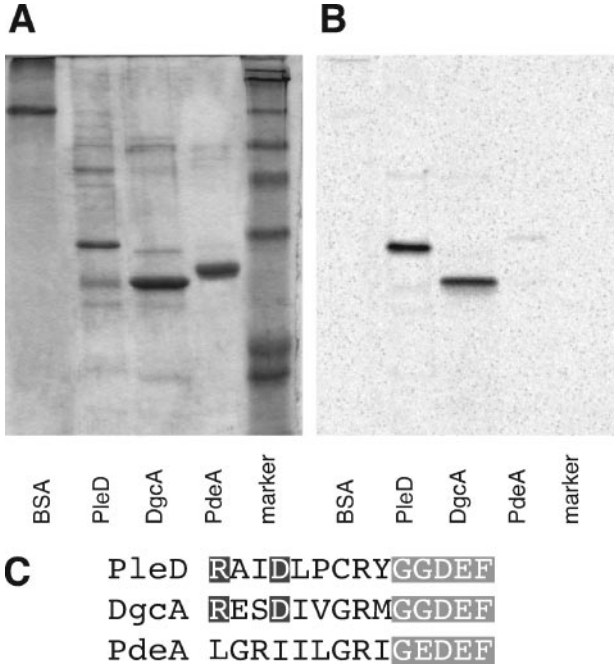

FIGURE 4. **UV cross-linking of different GGDEF domains with ^{33}P-labeled c-di-GMP.** *A*, Coomassie-stained SDS-PAGE and *B*, autoradiograph of BSA (control), PleDΔREC1, DgcA, and the isolated GGDEF domain of the c-di-GMP-specific phosphodiesterase PdeA (CC3396) after UV cross-linking with [^{33}P]c-di-GMP. *C*, alignment of I- and A-site sequence of PleD, DgcA, and PdeA. I-site (R*XX*D) and A-site residues (GGDEF) are marked in *black* and *gray*, respectively.

Evidence for an in Vivo Role of I-site-mediated Feedback Control—To test a possible role for feedback inhibition of diguanylate cyclases *in vivo*, we developed a simple assay based on the observation that in *E. coli* and other *Enterobacteriaceae* increased cellular levels of c-di-GMP correlate with Congo Red (CR) staining of colonies on plates (28). Low level expression (in the absence of the inducer IPTG) of active *pleD* alleles caused a red colony phenotype in the *E. coli* B strain BL21, whereas cells expressing inactive *pleD* alleles under the same conditions stained white (Fig. 3). Interestingly, PleD mutants with dramatically different diguanylate cyclase activities *in vitro* showed only minor differences of CR staining *in vivo*. For instance, PleDR148A/R178A, which showed a 20-fold increased activity (Table 1), or PleD*, a constitutively active mutant of PleD several 100-fold more active than wild-type (9), caused virtually identical CR values like PleD wild type (Fig. 3). In contrast, expression of the feedback inhibition mutant PleDR390A resulted in a significantly higher CR staining even though its *in vitro* DGC activity was lower than wild-type PleD (Table 1). This argued that *in vivo* steady-state concentrations of c-di-GMP were determined mainly by the PleD inhibition constant (as opposed to the overall activity of the enzyme) and that a functional I-site is critical for DGC control *in vivo*.

DgcA, a Single Domain Diguanylate Cyclase, Is Subject to Allosteric Product Inhibition—Sequence alignments of >1000 annotated GGDEF domain proteins revealed that that I-site residues Arg-359 and Asp-362 of PleD are highly conserved. 57% of the proteins containing a GGDEF domain and 27% of GGDEF/EAL composite proteins possess this motif. This suggested that c-di-GMP product inhibition could be a general regulatory mechanism of bacterial diguanylate cyclases. To test this, hexahistidine-tagged derivatives of two *C. crescentus* GGDEF domain proteins were analyzed biochemically with respect to their DGC activities and c-di-GMP binding properties. Purified DgcA (diguanylate cyclase A, CC3285), a soluble, single domain GGDEF protein that lacks an obvious N-terminal input domain, showed strong diguanylate cyclase activity (Fig. 5*A*). DgcA has an RESD motive five amino acids upstream of the conserved GGDEF active site and was readily labeled with [^{33}P]c-di-GMP in a cross-linking experiment (Fig. 4). Consistent with this, DgcA showed strong feedback inhibition (Fig. 5*A*) with its K_i (1 μM) being in the same range as the inhibition constant determined for PleD (8). In contrast, the GGDEF domain of PdeA (phosphodiesterase A, CC3396), which lacks catalytic activity (14), had no conserved I-site residues and did not bind radiolabeled c-di-GMP (Fig. 4). Thus, specific binding of c-di-GMP correlated with the presence of a conserved I-site motif R*XX*D (Fig. 4).

Diguanylate cyclase activity assays revealed strong and rapid product inhibition of DgcA. DgcA alone was able to convert only a small fraction of the available GTP substrate pool into the product c-di-GMP (V_o = 2.8 μmol of c-di-GMP μmol protein^{-1} min^{-1}) (Fig. 5*B*). In contrast, GTP consumption and conversion into c-di-GMP and pGpG was rapid (V_o = 43.0 μmol of c-di-GMP μmol protein^{-1} min^{-1}) and almost complete when the PDE CC3396 was added in excess to the enzymatic reaction (Fig. 5*B*). This argued that c-di-GMP feedback inhibition is abolished in a sequential DGC-PDE reaction, because the steady-state concentration of the inhibitor c-di-GMP is kept low by continuous degradation of c-di-GMP into the linear dinucleotide pGpG. As a consequence of rapid feedback inhibition, the experimentally determined V_o values of the DGC reaction are generally underestimated. In conclusion, these results strengthen the view that allosteric product inhibi-

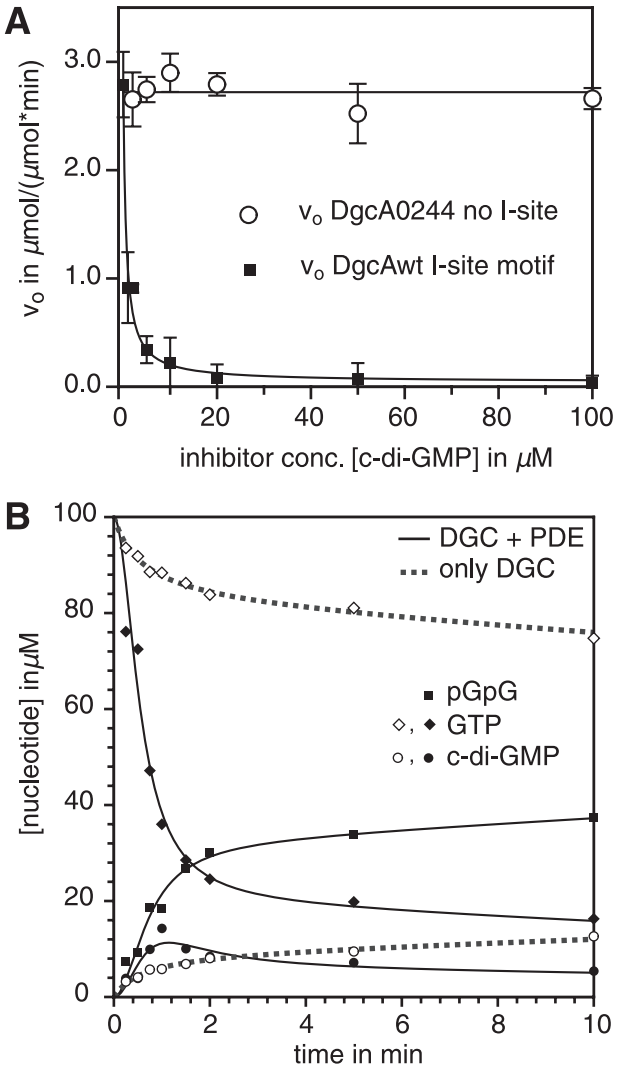

FIGURE 5. **c-di-GMP product inhibition of DgcA.** *A*, initial velocities of the wild-type diguanylate cyclase DgcA (*squares*) and the non-feedback inhibited I-site mutant DgcA0244 (*circles*) in the presence of increasing concentrations of c-di-GMP. *B*, conversion of GTP into c-di-GMP by DgcA (*dashed lines*) and accelerated GTP consumption, c-di-GMP synthesis, and cleavage into pGpG by a diguanylate cyclase-phosphodiesterase tandem reaction (*plain lines*).

tion is a general principle of diguanylate cyclases and that high affinity binding of c-di-GMP requires an R*XX*D I-site motif positioned in close proximity to the active site.

Development of an in Vivo Assay to Genetically Probe Allosteric Control of DgcA—DGCs from different bacterial species have been shown to be functionally interchangeable (17, 26, 27). To determine if DgcA is active *in vivo* we expressed a plasmid-based copy of the *dgcA* gene in *C. crescentus*, *S. enterica*, and *Escherichia coli* B and tested the respective strains for the phenotypes known to result from increased cellular levels of c-di-GMP (17, 26, 27). Consistent with these earlier findings, expression of *dgcA* strongly inhibited flagellar-based motility in all three organisms, dramatically increased the ability of *S. enterica* and *E. coli* for surface colonization, and produced the characteristic red, dry, and rough (rdar) colony morphotype when plated on CR plates (Fig. 6, *A–F*) (29). The red phenotype provided the basis for a visual genetic screen on CR plates. Under these conditions, cells producing active DgcA variants would produce dark red single colonies, whereas cells producing inactive DgcA mutants would remain white. This prompted us to use the CR screen to isolate *dgcA* mutants, which had a specific defect in feedback regulation, and to define the minimal requirements for product inhibition of this class of enzymes.

Randomization of c-di-GMP Binding Pocket Reveals Three Mutant Classes—To probe the minimal requirements of the I-site for c-di-GMP binding and product inhibition, a *dgcA* mutant library was constructed with the RESD signature replaced by a randomized tetrapeptide sequence (see "Materials and Methods"). In short, a *dgcA* gene, which carried a deletion of the four I-site codons, was used as template for a PCR reaction. For the amplification step a primer complementary to the 3′-end of *dgcA* was used in combination with a mixture of oligonucleotides that spanned the deletion site and contained 12 randomized base pairs at the position coding for the deleted amino acids. The resulting PCR fragments were fused in-frame with the 5′-end of *dgcA* in the expression plasmid pET42b and were transformed into *E. coli* BL21. The resulting gene library contains a theoretical number of 1.67×10^7 (4^{12}) different *dgcA* alleles, coding for DgcA variants with different combinations of I-site residues.

When plated on CR plates, colonies transformed with a wild-type *dgcA* allele showed the typical rdar colony morphology (Fig. 6*G*). Transformation of *E. coli* BL21 with a plasmid expressing a mutant DgcA, which lacked the four amino acids of the I-site (DgcAΔRESD), produced white colonies on CR plates (Fig. 6*H*), indicating that this mutant form had lost DGC activity. About 10% of the clones with random tetrapeptide insertions stained red on CR plates and thus had retained DGC activity (Fig. 6*I*). This result is consistent with the observation that alanine scanning of the PleD I-site almost exclusively produced non-active enzyme variants (Table 1) and argues that the majority of amino acid substitutions introduced at the I-site are detrimental for the catalytic activity of the DGC. To further characterize active DgcA I-site variants, a total of 800 red colonies was isolated and patched onto CR plates without (Fig. 6, *J* and *K*) or with the inducer IPTG (Fig. 6, *L* and M). This secondary screen was based on the observation that IPTG-induced expression of the *pleDR390A* allele (Table 1), but not of the *pleD* wild-type allele, abolished growth of *E. coli* BL21 (data not shown). This suggested that at elevated protein levels, DGCs that lack feedback control are toxic *in vivo* (see below). The majority of the I-site library clones tested failed to grow on plates containing IPTG, indicating that their activity is no longer controlled by product inhibition (Fig. 6, *L* and *M*). Only 7 mutants (out of 9000 colonies screened) showed a wild type-like behavior in that they stained dark red on CR plates and tolerated the presence of the inducer IPTG (Fig. 6, *L* and *M*).

This genetic screen led to the isolation of three different I-site mutant classes with the following characteristics: 1) catalytically inactive mutants (A^-, frequency ~90%); 2) feedback control negative mutants (I^-A^+, frequency ~10%); and wild-type-like mutants (I^+A^+, frequency ~0.1%). A subset of class 1 and 2 mutants and all seven class 3 mutants were selected, and hexahistidine-tagged forms of the respective proteins were purified for biochemical characterization. Kinetic parameters of activity (V_o) and feedback inhibition (K_i) were determined

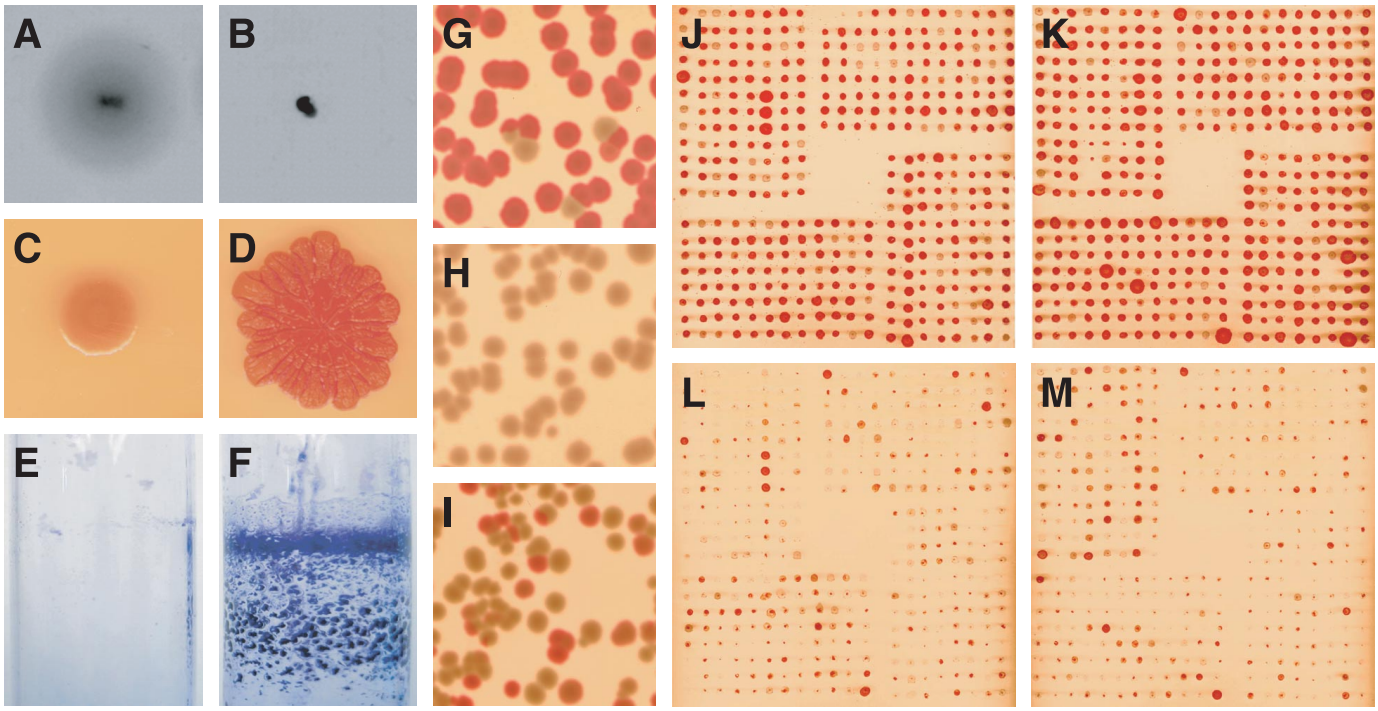

FIGURE 6. **Phenotypic characterization of ectopically expressed diguanylate cyclase *dgcA* in *E. coli* and *S. enterica*.** Behavior of *E. coli* strain BL21 with empty pET42b plasmid (*A*) and pET42b::*dgcA* (*B*) on motility plates. Colony morphology of *E. coli* strain BL21 with empty pET42b plasmid (*C*) and with pET42b::*dgcA* (*D*) on Congo Red plates. Biofilm formation of *S. enterica* serovar Typhimurium *trp*::*T7RNAP* with empty pET42b (*E*) and pET42b::*dgcA* (*F*) grown in liquid culture and stained with crystal violet. *E. coli* BL21 transformed with PCR-restored *dgcA* wild type on pET42b::*dgcA* (*G*), with the inactive allele *dgcA*ΔRESD (pET42b::*dgcA*ΔRESD) (*H*), and with a library of random tetrapeptide insertions in the I-site (pET42b::*dgcA*XXXX) (*I*) and plated on Congo Red plates. *E. coli* BL21 expressing different I-site mutant alleles were spotted onto Congo Red plates without (*J* and *K*) and with 1 mM IPTG (*L* and *M*) to screen for feedback inhibition *dgcA* alleles.

TABLE 1
Kinetic analysis of PleD mutants

Protein	V_o	ΔV_o	K_i	ΔK_i
	*μmol c-di-GMP/ (μmol protein*min)*		*μM*	
PleD wild type	0.202	± 0.023	5.8	± 1.0
PleDR359A	0.005	ND[a]	>100	ND
PleDR359V	0.0	ND		
PleDΔ359Δ362	0.0	ND		
PleDD362A	0.0	ND		
PleDR390A	0.076	± 0.007	115.0	± 18.1
PleDR148A	0.822	± 0.020	2.8	± 1.2
PleDR178A	0.918	± 0.292	3.6	± 0.1
PleDR148AR178A	3.75	± 0.43	2.9	± 0.6
PleDG194W	0.161	± 0.005	6.3	± 1.9
PleDEE370GG	0.0	ND		
PleDE370Q	0.0	ND		
PleDE371Q	0.0	ND		

[a] ND, not determined.

individually using an *in vitro* diguanylate cyclase activity assay (16). Consistent with their rdar-like *in vivo* phenotype, only class 2 and class 3 mutants showed detectable diguanylate cyclase activity with an initial velocity between 1.93 and 14.21 μmol of c-di-GMP μmol protein^{-1} min^{-1} (Table 2). Only mutant proteins from the IPTG tolerant class 3 showed product inhibition with K_i values close to 1 μM (Table 2). In contrast, all proteins from class 2 mutants showed no feedback inhibition *in vitro*, arguing that their *in vivo* toxicity is the result of uncontrolled run-off DGC activity (Fig. 5*A* and Table 2). Support for this hypothesis comes from experiments determining the cellular concentration of c-di-GMP and DgcA protein expression levels in *E. coli* BL21 carrying selected *dgcA* alleles on plasmid pET42b (see "Materials and Methods"). Alleles *dgcA0244*, *dgcA1229*, and *dgcA1250* were chosen, because the DGC activity of these enzymes is similar to wild type DgcA (Table 2). Basal level expression (no IPTG) of *dgcA0244*, the allele coding for a DGC that completely lacks feedback inhibition, resulted in a more than 100-fold increased cellular level of c-di-GMP as compared with cells expressing wild-type *dgcA* (Table 3). This was due to an almost 100-fold higher overall turnover of the mutant enzyme as compared with wild type (Table 3). In contrast, enzymatic turnover and cellular concentration of c-di-GMP was increased only marginally in *E. coli* cells expressing alleles *dgcA1229*, and *dgcA1250* with restored feedback inhibition control (Table 3).

Sequence analysis of the tetrapeptide insertions of class 2 and class 3 mutants revealed several important characteristics of a functional allosteric I-site binding pocket. All catalytically active and feedback inhibition competent mutants restored the wild-type Arg and Asp residues at positions one and four of the *RXXD* motive (Table 2). Whereas most of the mutants that had lost feedback inhibition had altered either one or both of these charged residues (Table 2) only two feedback inhibition mutants had retained both charges with changes in the intervening residues (Table 2). Obviously, Arg and Asp, while being strictly required for feedback inhibition, need to be placed in the appropriate sequence context of the I-site loop. These experiments define the minimal requirements of the I-site core region and demonstrate that the Arg and Asp residues that make direct contacts to the c-di-GMP ligand in the crystal structure are of critical functional importance for DGC feedback inhibition *in vivo* and *in vitro*. This provides a plausible

TABLE 2
Diguanylate cyclase activity and inhibition constant of DgcA I-site mutant proteins

Protein	Motif	V_o	ΔV_o	K_i	ΔK_i
		μmol c-di-GMP/ (μmol protein·min)		*μM*	
DgcA wt	RESD	2.79	± 0.01	0.96	± 0.09
DgcA1406	RQGD	5.35	± 0.05	7.02	± 2.92
DgcA1040	RLVD	4.92	± 0.19	4.52	± 1.81
DgcA1229	RGAD	2.03	± 0.01	1.84	± 0.26
DgcA1524	RSAD	3.70	± 0.13	7.36	± 2.69
DgcA1529	RLAD	2.79	± 0.04	1.01	± 0.23
DgcA0751	RCAD	3.65	± 0.10	3.51	± 0.52
DgcA1250	RGGD	2.07	± 0.02	2.24	± 0.49
DgcAΔRESD		0.14	± 0.06	ND[a]	
DgcA0207	GMGG	14.21	± 0.54	No inhibition	
DgcA0244	VMGG	2.57	± 0.05	No inhibition	
DgcA0613	GGVA	4.29	± 0.06	No inhibition	
DgcA0646	GRDC	8.90	± 0.10	No inhibition	
DgcA0913	GVGD	3.81	± 0.04	No inhibition	
DgcA1300	MEGD	0.87	± 0.02	No inhibition	
DgcA1733	GGNH	11.47	± 0.17	No inhibition	
DgcA3018	RESE	11.1	± 0.11	No inhibition	
DgcA0230	RNRD	3.02	± 0.06	No inhibition	
DgcA0642	RVDS	4.17	± 0.08	No inhibition	
DgcA1007	RAGG	6.06	± 0.05	No inhibition	
DgcA2006	RGQD	1.93	± 0.01	No inhibition	

[a] ND, not determined.

TABLE 3
DgcA protein levels and cellular c-di-GMP concentrations in the absence or presence of IPTG induction at 1 mM

	Protein conc.[a]		c-di-GMP conc.		Turnover[b]	
	No induction	1 mM IPTG	No induction	1 mM IPTG	No induction	1 mM IPTG
	pmol protein/mg dry weight		*pmol c-di-GMP/mg dry weight*		*pmol c-di-GMP per pmol protein*	
DgcA0244	4.1	22	1466.3	1570.7	357.6	71.4
DgcA1229	3.5	31	87.6	139.5	25.0	4.5
DgcA1250	2.7	43	24.2	305.4	9.0	7.1
DgcA wt	2.9	33	13.75	189.4	4.7	5.7
DgcAΔRESD	3.5	23	ND[c]	ND	NA[d]	NA

[a] See "Materials and Methods."
[b] As derived from the cellular c-di-GMP concentration divided by the cellular protein concentration.
[c] ND, not detectable.
[d] NA, not applicable.

explanation for the strong conservation of the R*XX*D motif in GGDEF domains.

The molecular mechanism of product inhibition through I-site binding remains unclear. To assist the interpretation of the present data and provide information on binding induced mobility, atomistically detailed simulations were carried out. Normal mode calculations on ligated and unligated PleD were used to analyze the structural transitions that occur during I-site binding of c-di-GMP. Normal mode calculations on the optimized structures yielded no imaginary frequencies, and translational and rotational frequencies were close to zero ($|\omega| \leq 0.02\ cm^{-1}$). This indicated that the minimized structures correspond to real minima on the potential energy surface. The displacements calculated for the ligated and the unligated protein showed a significant decrease in mobility for both I- and A-site residues upon complexation (supplemental Figs. S2 and S3). Whereas motion in the I-site is suppressed due to steric interactions upon ligand insertion, quenching of the A-site residues suggested that the two sites might be dynamically coupled via the short connecting β-strand (β2). Backbone Cα-atoms and side chains of the I-site and A-site loops were displaced by an average of 1–4 Å in opposite directions, arguing that a balance-like movement centered around β2 could be responsible for direct information transfer between the two sites (Fig. 7). The cumulated displacements per residue over all 147 modes (supplemental Fig. S3) showed different mobilities in additional regions of the protein. The Cα atoms of residues exhibiting large changes in flexibility upon ligand binding are depicted as *spheres* in supplemental Fig. S3. Reduced flexibility (*yellow spheres*) is found at the I-site, A-site, phosphorylation site, and the dimer interface, whereas the flexibility is enhanced (*black spheres*) at the REC1/REC2 interface. In summary, these simulations show that I-site binding of c-di-GMP not only reduced the mobility around the R*XX*D motif but also of the residues of the A-site loop.

DISCUSSION

Feedback Inhibition Is a General Control Mechanism of Diguanylate Cyclases—The data presented here propose a general mechanism to regulate the activity of diguanylate cyclases (DGCs), key enzymes of c-di-GMP-based signal transduction in bacteria. High affinity binding of c-di-GMP to a site distant from the catalytic pocket (I-site) efficiently blocks enzymatic activity in a non-competitive manner. Mutational analysis of multi- and single-domain DGC proteins has provided convincing evidence for the role of several charged amino acids in c-di-GMP binding and allosteric regulation. Furthermore, these experiments indicated that the allosteric binding site is functionally contained within the GGDEF domain. An *in vivo* selection experiment using a random tetrapeptide library, and

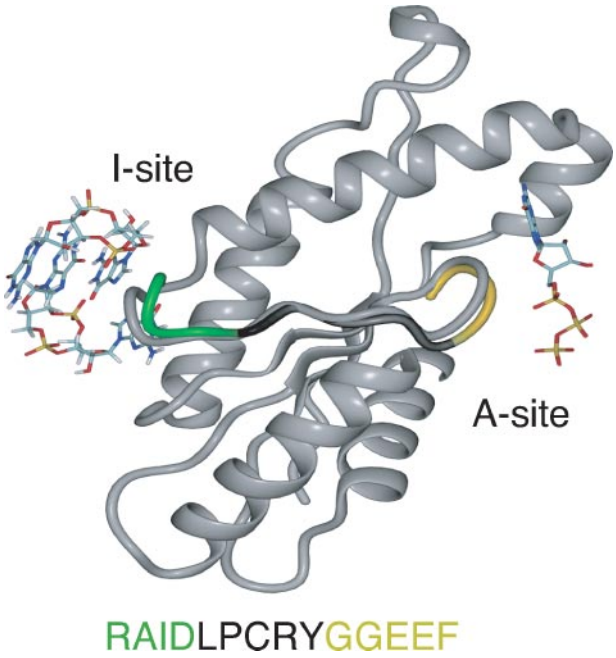

FIGURE 7. **Comparison of the energy-minimized structures of the PleD GGDEF domain with and without ligand bound to the I-site.** For improved clarity, the domain is sliced through the I-site loop/β2/A-site loop plane. The unligated protein is shown in *gray* and the I-site loop (*green*), β2 (*black*), and A-site loop (*gold*) of the bound structure are shown as an overlay. GTP bound to the active site is modeled according to the orientation of c-di-GMP bound to the A-site in the crystal structure. The PleD amino acid sequence of I-site, β2, and A-site is indicated below.

designed to re-engineer the I-site has led to the definition of a highly conserved R*XX*D core motif of the c-di-GMP binding pocket. The R*XX*D motif forms a turn at the end of a short five-amino acid β-sheet that directly connects the I-site with the conserved catalytic A-site motif, GG(D/E)EF (Fig. 7). This raised the question of how I-site ligand binding modulates DGC enzyme activity. In the multidomain protein PleD, c-di-GMP bound to the I-site physically connects the GGDEF domain with the REC1-REC2 dimerization stem. It was speculated that product inhibition occurs by domain immobilization, which would prevent the encounter of the two DGC substrate binding sites (8). Several observations argue in favor of a more direct communication between I- and A-sites. First, with a large variety of domains found to be associated with GGDEF domains, it seems unlikely that functional I-sites are generally formed by the interface of a GGDEF with its neighboring domain (2). In agreement with this, residues of the PleD REC2 domain are not required for c-di-GMP binding and feedback inhibition. Second, the single domain DGC protein, DgcA, shows I-site-dependent allosteric control with a K_i of 1 μM. Third, the introduction of a bulky tryptophan residue (G194W) at the GGDEF-REC2 interface did not affect activity, I-site binding, or feedback inhibition of PleD (Fig. 2 and Table 1). Fourth, atomistic simulations of ligated and unligated PleD predicted a marked drop in flexibility of Cα-atoms both in the I- and A-site upon ligand binding. Simultaneous with motion quenching, β2 and its flanking I- and A-loops undergo a balance-like movement that repositions A-site residues in the catalytic active site (Fig. 7). This is consistent with the idea that structural changes within the GGDEF domain upon binding of c-di-GMP at the I-site lead to repositioning of active site residues and possibly altered kinetic parameters. Thus, we propose that c-di-GMP binding and allosteric control represents an intrinsic regulatory property of DGCs that contain an R*XX*D motif.

Like guanylate and adenylate cyclases (GCs and ACs) and DNA polymerases, DGCs catalyze the nucleophilic attack of the 3′-hydroxyl group on the α-phosphate of a nucleoside triphosphate. Despite the lack of obvious sequence similarities, the PleD x-ray structure revealed that DGCs possess a similar domain architecture like ACs and GCs (8, 30). Based on mutational analysis (8, 14, 16) and on structural comparisons between DGC, AC, GC, and DNA polymerases (31–34), a model for DGC catalysis can be proposed. In contrast to the heterodimeric ACs and GCs, DGCs form homodimers, with a GTP molecule bound within the catalytic core of each DGC monomer (8). Two Mg^{2+} ions are coordinated by the highly conserved glutamic acid residue Glu-371, which is part of the GGDEF motif, and possibly by Asp-327 on the opposing β-sheet. The divalent Mg^{2+} carboxyl complex coordinates the triphosphate moiety of GTP and activates the 3′-hydroxyl group for intermolecular nucleophilic attack. Substrate specificity of AC and GC can be interchanged by converting a few key residues involved in purine recognition (31, 34, 35). This includes an arginine residue, which in PleD corresponds to the highly conserved Arg-366 located in the β-sheet connecting the I- and A-sites. Based on the active site model, two alternative inhibition mechanisms can be envisaged. In a first scenario, binding of c-di-GMP to the I-site would change the orientation of Arg-366 and would thereby disturb the guanine binding pocket resulting in an increased K_m for GTP. Alternatively, inhibitor binding could rearrange the Mg^{2+} carboxyl complex and thus destabilize the active state.

In Silico Analysis of the GGDEF Protein Family Indicates That Product Inhibition Is a General Regulatory Mechanism—DGC activity of GGDEF domain proteins seems to strictly depend on conserved GGDEF or GGEEF motifs in the active site (10, 16, 18, 36–38). Consistent with this, ~90% of the GGDEF and 62% of the GGDEF/EAL composite proteins show a conserved GG(D/E)EF A-site motif. Of the GGDEF proteins with a highly conserved A-site motif, >60% have conserved R*XX*D I-site residues and a conserved spacer length between I- and A-site, arguing that the three-dimensional arrangement of catalytic and allosteric pocket is likely to be similar in all DGCs. From a total of 19 GGDEF proteins, for which convincing evidence for a DGC activity exists, 14 have a conserved I-site (supplemental Fig. S4). Ryjenkov and coworkers (10) reported severe toxicity problems when expressing diguanylate cyclases lacking I-site residues in *E. coli* BL21. This is consistent with the growth defect observed upon expression of *dgcA* feedback inhibition mutants in *E. coli* BL21 and argues that these proteins are not feedback-controlled. The molecular basis of growth interference under these conditions is unclear. It is possible that depletion of the GTP pool or adverse effects of unphysiologically high levels of c-di-GMP are responsible for this effect. Although the experiments presented here define a role for the I-site in DGC feedback inhibition, the c-di-GMP binding pocket could also be exploited for other roles in c-di-GMP signaling. It has been proposed recently that non-catalytic GGDEF

domains with variant A-site motifs can fulfill regulatory functions (14). It is attractive to speculate that a subgroup of GGDEF proteins that has degenerate catalytic A-sites but conserved c-di-GMP binding pockets, represents a novel class of c-di-GMP effector proteins that regulate cellular functions in response to c-di-GMP binding.

Regulatory Significance of DGC Feedback Control—GGDEF domains are often associated with sensory domains in one- or two-component signaling systems (39, 40). Thus it is reasonable to assume that in most cases DGC activity is controlled by direct signal input through these domains. But why then would a substantial portion of these enzymes also be subject to feedback inhibition? There are several possibilities, which among themselves are not mutually exclusive. Given the anticipated regulatory complexity of the c-di-GMP signaling network (2, 39) and the potentially dramatic changes in cellular physiology and behavior caused by fluctuating levels of c-di-GMP, it is in the cell's best interest to rigorously control the production of the second messenger. Product inhibition of DGCs allows the establishment of precise threshold concentrations of the second messenger, or, in combination with counteracting PDEs, could produce short spikes or even generate oscillations of c-di-GMP. In addition, negative feedback loops have been implicated in neutralizing noise and providing robustness in genetic networks by limiting the range over which the concentrations of the network components fluctuate (41, 42). Similarly, product inhibition of DGCs could contribute to the reduction of stochastic perturbations and increase the stability of the c-di-GMP circuitry by keeping c-di-GMP levels in defined concentration windows. Alternatively, DGC autoregulation may influence the kinetics of c-di-GMP signaling. Mathematical modeling and experimental evidence suggested that negative autoregulation in combination with strong promoters substantially shortens the rise-time of transcription responses (43–45). In analogy, a desired steady-state concentration of c-di-GMP can in principle be achieved by two regulatory designs: (*a*) a low activity DGC with no product inhibition, and (*b*) a high activity DGC with built-in negative autoregulation. In cases where circuits have been optimized for fast up-kinetics, design B will be superior. It is plausible that DGCs with or without I-site motifs can be divided into these two kinetically different classes.

This study contributes to the emerging understanding of the c-di-GMP regulatory network in bacteria. The current emphasis lies on the identification of effector molecules, regulatory mechanisms, and processes controlled by c-di-GMP. With the long term goal in mind of approaching a detailed systems-level understanding of c-di-GMP signaling, kinetic parameters of signaling mechanisms will require our particular attention. Our experiments provide an entry point into the kinetic analysis of individual DGCs and the quantitative assessment of the c-di-GMP circuitry.

Acknowledgments—We thank Tilman Schirmer for helpful discussions and students of the Microbiology and Immunology Course (Biozentrum of the University of Basel, 2005) and of the Advanced Bacterial Genetics Course (Cold Spring Harbor, 2005) for their help in mutant screening.

REFERENCES

1. Jenal, U. (2004) *Curr. Opin. Microbiol.* **7,** 185–191
2. Romling, U., Gomelsky, M., and Galperin, M. Y. (2005) *Mol. Microbiol.* **57,** 629–639
3. Brouillette, E., Hyodo, M., Hayakawa, Y., Karaolis, D. K. R., and Malouin, F. (2005) *Antimicrob. Agents Chemother.* **49,** 3109–3113
4. Hisert, K. B., MacCoss, M., Shiloh, M. U., Darwin, K. H., Singh, S., Jones, R. A., Ehrt, S., Zhang, Z. Y., Gaffney, B. L., Gandotra, S., Holden, D. W., Murray, D., and Nathan, C. (2005) *Mol. Microbiol.* **56,** 1234–1245
5. Kulesekara, H., Lee, V., Brencic, A., Liberati, N., Urbach, J., Miyata, S., Lee, D. G., Neely, A. N., Hyodo, M., Hayakawa, Y., Ausubel, F. M., and Lory, S. (2006) *Proc. Natl. Acad. Sci. U. S. A.* **103,** 2839–2844
6. Lestrate, P., Dricot, A., Delrue, R. M., Lambert, C., Martinelli, V., De Bolle, X., Letesson, J. J., and Tibor, A. (2003) *Infect. Immun.* **71,** 7053–7060
7. Tischler, A. D., Lee, S. H., and Camilli, A. (2002) *J. Bacteriol.* **184,** 4104–4113
8. Chan, C., Paul, R., Samoray, D., Amiot, N. C., Giese, B., Jenal, U., and Schirmer, T. (2004) *Proc. Natl. Acad. Sci. U. S. A.* **101,** 17084–17089
9. Ross, P., Weinhouse, H., Aloni, Y., Michaeli, D., Weinbergerohana, P., Mayer, R., Braun, S., Devroom, E., Vandermarel, G. A., Vanboom, J. H., and Benziman, M. (1987) *Nature* **325,** 279–281
10. Ryjenkov, D. A., Tarutina, M., Moskvin, O. V., and Gomelsky, M. (2005) *J. Bacteriol.* **187,** 1792–1798
11. Ross, P., Mayer, R., and Benziman, M. (1991) *Microbiol. Rev.* **55,** 35–58
12. Schmidt, A. J., Ryjenkov, D. A., and Gomelsky, M. (2005) *J. Bacteriol.* **187,** 4774–4781
13. Tamayo, R., Tischler, A. D., and Camilli, A. (2005) *J. Biol. Chem.* **280,** 33324–33330
14. Christen, M., Christen, B., Folcher, M., Schauerte, A., and Jenal, U. (2005) *J. Biol. Chem.* **280,** 30829–30837
15. Tal, R., Wong, H. C., Calhoon, R., Gelfand, D., Fear, A. L., Volman, G., Mayer, R., Ross, P., Amikam, D., Weinhouse, H., Cohen, A., Sapir, S., Ohana, P., and Benziman, M. (1998) *J. Bacteriol.* **180,** 4416–4425
16. Paul, R., Weiser, S., Amiot, N. C., Chan, C., Schirmer, T., Giese, B., and Jenal, U. (2004) *Genes Dev.* **18,** 715–727
17. Aldridge, P., Paul, R., Goymer, P., Rainey, P., and Jenal, U. (2003) *Mol. Microbiol.* **47,** 1695–1708
18. Kirillina, O., Fetherston, J. D., Bobrov, A. G., Abney, J., and Perry, R. D. (2004) *Mol. Microbiol.* **54,** 75–88
19. Aldridge, P., and Jenal, U. (1999) *Mol. Microbiol.* **32,** 379–391
20. Hecht, G. B., and Newton, A. (1995) *J. Bacteriol.* **177,** 6223–6229
21. Ely, B. (1991) *Methods Enzymol.* **204,** 372–384
22. O'Toole, G. A., Pratt, L. A., Watnick, P. I., Newman, D. K., Weaver, V. B., and Kolter, R. (1999) *Methods Enzymol.* 34, 586–595
23. Ochi, Y., Hosoda, S., Hachiya, T., Yoshimura, M., Miyazaki, T., and Kajita, Y. (1981) *Acta Endocrinol.* **98,** 62–67
24. Brooks, B. R., Bruccoleri, R. E., Olafson, B. D., States, D. J., Swaminathan, S., and Karplus, M. (1983) *J. Comput. Chem.* **4,** 187–217
25. MacKerell, A. D., Bashford, D., Bellott, M., Dunbrack, R. L., Evanseck, J. D., Field, M. J., Fischer, S., Gao, J., Guo, H., Ha, S., Joseph-McCarthy, D., Kuchnir, L., Kuczera, K., Lau, F. T. K., Mattos, C., Michnick, S., Ngo, T., Nguyen, D. T., Prodhom, B., Reiher, W. E., Roux, B., Schlenkrich, M., Smith, J. C., Stote, R., Straub, J., Watanabe, M., Wiorkiewicz-Kuczera, J., Yin, D., and Karplus, M. (1998) *J. Phys. Chem. B* **102,** 3586–3616
26. Ausmees, N., Mayer, R., Weinhouse, H., Volman, G., Amikam, D., Benziman, M., and Lindberg, M. (2001) *FEMS Microbiol. Lett.* **204,** 163–167
27. Simm, R., Fetherston, J. D., Kader, A., Romling, U., and Perry, R. D. (2005) *J. Bacteriol.* **187,** 6816–6823
28. Garcia, B., Latasa, C., Solano, C., Portillo, F. G., Gamazo, C., and Lasa, I. (2004) *Mol. Microbiol.* **54,** 264–277
29. Zogaj, X., Nimtz, M., Rohde, M., Bokranz, W., and Romling, U. (2001) *Mol. Microbiol.* **39,** 1452–1463
30. Pei, J., and Grishin, N. V. (2001) *Proteins* **42,** 210–216
31. Tucker, C. L., Hurley, J. H., Miller, T. R., and Hurley, J. B. (1998) *Proc. Natl. Acad. Sci. U. S. A.* **95,** 5993–5997
32. Zhang, G. Y., Liu, Y., Ruoho, A. E., and Hurley, J. H. (1997) *Nature* **388,** 204 (Errratum)

33. Tesmer, J. J., Sunahara, R. K., Johnson, R. A., Gosselin, G., Gilman, A. G., and Sprang, S. R. (1999) *Science* **285,** 756–760
34. Sunahara, R. K., Beuve, A., Tesmer, J. J. G., Sprang, S. R., Garbers, D. L., and Gilman, A. G. (1998) *J. Biol. Chem.* **273,** 16332–16338
35. Baker, D. A., and Kelly, J. M. (2004) *Mol. Microbiol.* **52,** 1229–1242
36. Hickman, J. W., Tifrea, D. F., and Harwood, C. S. (2005) *Proc. Natl. Acad. Sci. U. S. A.* **102,** 14422–14427
37. Mendez-Ortiz, M. M., Hyodo, M., Hayakawa, Y., and Membrillo-Hernandez, J. (2006) *J. Biol. Chem.* **281,** 8090–8099
38. Simm, R., Morr, M., Kader, A., Nimtz, M., and Romling, U. (2004) *Mol. Microbiol.* **53,** 1123–1134
39. Galperin, M. Y., Nikolskaya, A. N., and Koonin, E. V. (2001) *FEMS Microbiol. Lett.* **204,** 213–214
40. Ulrich, L. E., Koonin, E. V., and Zhulin, I. B. (2005) *Trends Microbiol.* **13,** 52–56
41. Becskei, A., and Serrano, L. (2000) *Nature* **405,** 590–593
42. Gardner, T. S., Cantor, C. R., and Collins, J. J. (2000) *Nature* **403,** 339–342
43. McAdams, H. H., and Arkin, A. (1997) *Proc. Natl. Acad. Sci. U. S. A.* **94,** 814–819
44. Rosenfeld, N., Elowitz, M. B., and Alon, U. (2002) *J. Mol. Biol.* **323,** 785–793

SUPPLEMENTAL MATERIAL:

MATERIALS AND METHODS:

Purification of His-tagged proteins - E. coli BL21 cells carrying the respective expression plasmid were grown in LB medium with ampicillin (100μg/ml) or kanamycin (30μg/ml) and expression was induced by adding IPTG at OD_{600} 0.4 to a final concentration of 0.4 mM. After harvesting by centrifugation, cells were resuspended in buffer containing 50 mM Tris-HCl, pH 8.0, 250 mM NaCl, 5 mM β-mercaptoethanol, lysed by passage through a French pressure cell, and the suspension was clarified by centrifugation for 10 min at 5,000 x g. Soluble and insoluble protein fractions were separated by a high-spin centrifugation step (100,000 x g, 1 h). The supernatant was loaded onto Ni-NTA affinity resin (Qiagen), washed with buffer, and eluted with an imidazol-gradient as recommended by the manufacturer. Protein preparations were examined for purity by SDS-PAGE and fractions containing pure protein were pooled and dialyzed for 12 h at 4°C.

Molecular modeling of PleD

All-atom simulations were carried out using the CHARMM (25) program and the CHARMM22/27 force field (26). The A chain of the X-ray dimer structure (PDB entry: 1W25 (17)) was used. All titratable side chains were generated in their standard protonation state at pH 7. Parameters and partial charges for the non-standard residue c-di-GMP were adopted from the extended CHARMM parameter sets for nucleic acids. The structure of the ligated (intercalated c-di-GMP bound to the I-site) and the unligated protein, to which hydrogen atoms were added, were minimized using a distance-dependent dielectric with ε=4 and a cutoff of 12 Å for non-bonded interactions. 5000 steps of steepest descent minimization were followed by adopted Newton Raphson minimization until a RMS gradient of 10^{-7} kcal/mol·Å was reached. Such a threshold is found to be sufficient for normal mode calculations (49). Normal modes were calculated with the diagonalization in a mixed basis (DIMB) method, as implemented in CHARMM. The DIMB method is an approximate scheme retaining the full atomistic description of the protein, where the Hessian is approximated iteratively. The total number of basis functions was 153 and cumulated displacements were calculated for T = 300 K.

For ligated PleD motion is suppressed at L(β1,α1) (res.10-12), L(β3,α3) domain REC1, the C-terminal end of α3 (res. 220-224) of domain REC2, the unstructured linker between REC2 and GGDEF domain (res. 282-284), the residues forming the A-site (res. 352), L(α2,β2) (res. 357-

360, I-site), L(β2,β3) (res. 367-373, A-site) and at the C-terminal end of α3 (res. 396-398) of the GGDEF domain. By contrast upon ligand binding mobility increases for α1 (res. 24), α4 (res. 96-99) of domain REC1, residues (res. 149, 175), L(β2,α2) (res. 205-207), L(β5,α5) (res. 254-257) of domain REC2 and residues L(β3',β3'') (res. 404-407) and L(β4,α4) (res. 422-424) of the GGDEF domain.

Primer list

The following primers were used: #1006, ACA CGC TAC ATA TGA AAA TCT CAG GCG CCC GGA C; #1007, ACT CTC GAG AGC GCT CCT GCG CTT; #1129, CAA GCG GCT GCA GGC CAA TGT GAT CGT CGG CCG CAT GGG TGG TGA; #670, TGC TAG TTA TTG CTC AGC GG; #1006 ACA CGC TAC ATA TGA AAA TCT CAG GCG CCC GGA C; #1130, CAA GCG GCT GCA GGC CAA TGT GCG CGA AAG CGA CAT CGT CGG CCG CAT GGG TGG TGA; #1132, CAC ATT GGC CTG CAG CCG CTT GGC GAC; #1131, CAA GCG GCT GCA GGC CAA TGT GNN NNN NNN NNN NAT CGT CGG CCG CAT GGG TGG TGA.

FIGURE LEGENDS:

Figure S1: **Separation of peptides yielded from tryptic digest of PleD in the presence (red chromatogram) or absence of c-di-GMP (black chromatogram) on a C18 column.** Peaks identified by ESI-MS: c-di-GMP m/z 691, t_R 7.70 min, T47 (amino acids 354-359) m/z 659.3 t_R 25.64 min. T49 (amino acids 367-386) m/z 2167.7 t_R 47.73 min.

Figure S2: **Normal modes of PleD I-site and A-site residues.** The displacements for each mode of the ligated and unligated structures are shown in Å for the residues of the REC2 domain (green) and the GGDEF domain (red). Insertion of intercalated c-di-GMP in the I-site quenches motion in both the I-site (R359-D362, R390) and the A-site (G368-E371), suggesting that the two sites are dynamically coupled.

Figure S3: **Representation of the PleD protein (blue: REC1, green: REC2, red: DGC) with c-di-GMP bound to the I-site.** Cα-atoms at positions of considerable changes in flexibility upon ligand binding are shown as spheres; reduced flexibility (yellow) and enhanced flexibility (black). Note that binding of c-di-GMP at the I-site (I) affects mobility not only in the I-site, but also in other regions of the protein, e.g. A-site (A), phosphorylation site (P) and dimer interface.

Figure S4: **Alignment of I- and A-site sequence of biochemically characterized diguanylate cyclases.** I-site residues (RXXD) are underlined in green and A-site residues (GGDEF) are underlined in yellow.

FIGURE LEGENDS:

Figure S1: **Separation of peptides yielded from tryptic digest of PleD in the presence (red chromatogram) or absence of c-di-GMP (black chromatogram) on a C18 column.** Peaks identified by ESI-MS: c-di-GMP m/z 691, t_R 7.70 min, T47 (amino acids 354-359) m/z 659.3 t_R 25.64 min. T49 (amino acids 367-386) m/z 2167.7 t_R 47.73 min.

Figure S2: **Normal modes of PleD I-site and A-site residues.** The displacements for each mode of the ligated and unligated structures are shown in Å for the residues of the REC2 domain (green) and the GGDEF domain (red). Insertion of intercalated c-di-GMP in the I-site quenches motion in both the I-site (R359-D362, R390) and the A-site (G368-E371), suggesting that the two sites are dynamically coupled.

Figure S3: **Representation of the PleD protein (blue: REC1, green: REC2, red: DGC) with c-di-GMP bound to the I-site.** Cα-atoms at positions of considerable changes in flexibility upon ligand binding are shown as spheres; reduced flexibility (yellow) and enhanced flexibility (black). Note that binding of c-di-GMP at the I-site (I) affects mobility not only in the I-site, but also in other regions of the protein, e.g. A-site (A), phosphorylation site (P) and dimer interface.

Figure S4: **Alignment of I- and A-site sequence of biochemically characterized diguanylate cyclases.** I-site residues (RXXD) are underlined in green and A-site residues (GGDEF) are underlined in yellow.

Figure S1

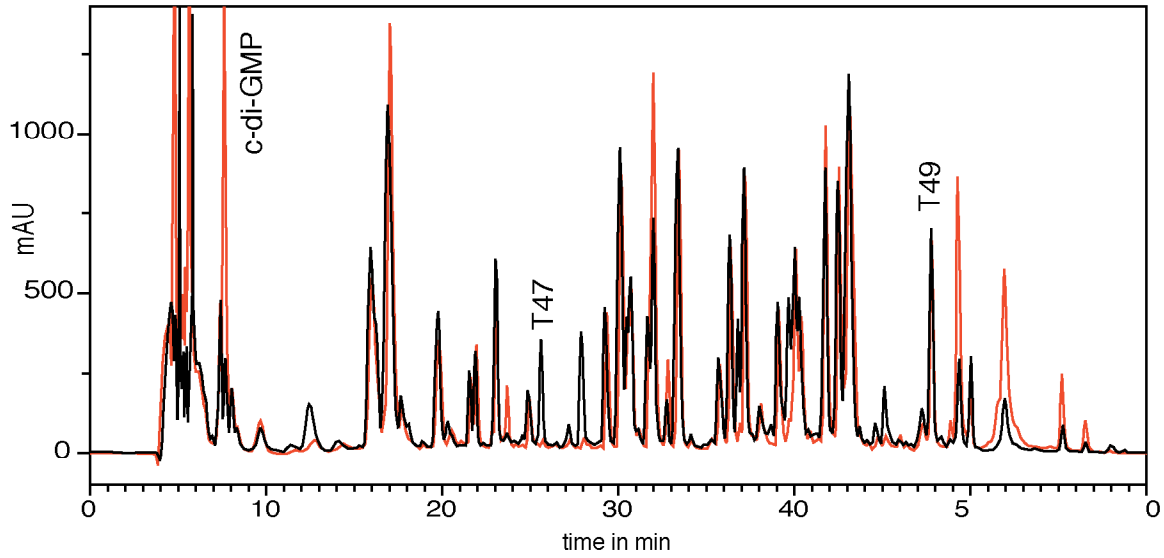

Figure S2

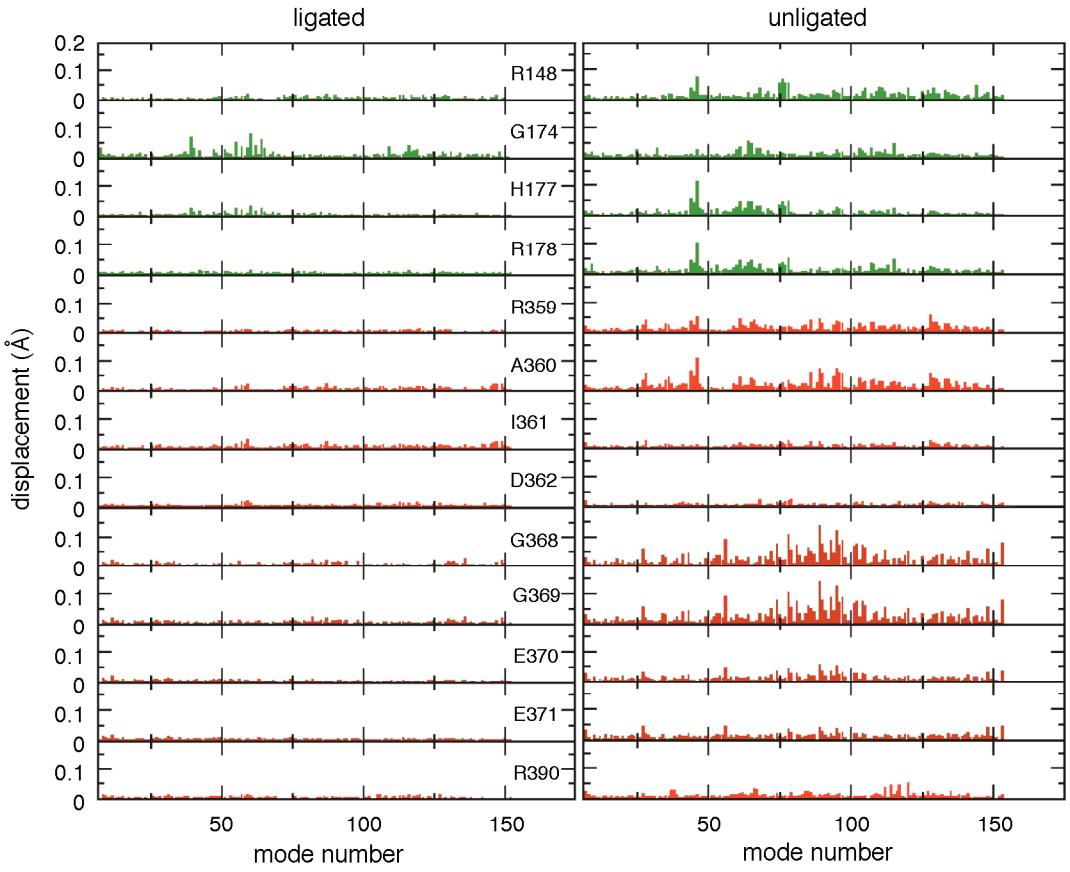
ligated
unligated
displacement (Å)
R148
G174
H177
R178
R359
A360
I361
D362
G368
G369
E370
E371
R390
0.2
0.1
0
50
100
150
mode number

Figure S3

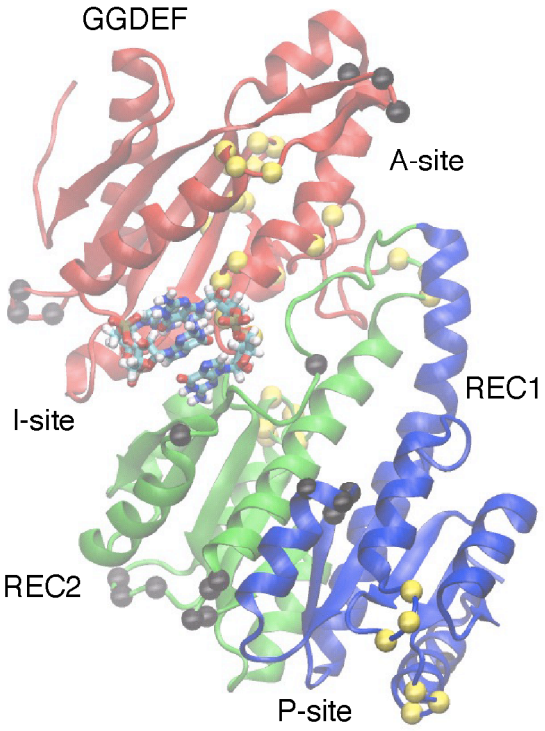

Figure S4

Gene	Sequence	Reference
BORBU_BB0419	LKYKIDVARYGGEEFI	(Ryjenkov et al, 2005)
CAUCR_DgcA	VRESDIVGRMGGDEFA	- this study
CAUCR_PleD	VRAIDLPCRYGGEEFV	(Paul et al, 2004)
DEIRA_DRB0044	LPGGASLYRVGGDEFV	(Ryjenkov et al, 2005)
ECOLI_YddV	VRSSDYVFRYGGDEFI	(Mendez-Ortiz, 2006)
ECOLI_YeaP	QQNGEVIGRLGGDEFL	(Ryjenkov et al, 2005)
PSEAE_PA1107	TRSSDSVARLGGEEFL	(Kulesekara et al, 2006)
PSEAE_PA1120	LRESDLVARLGGDEFA	(Kulesekara et al, 2006)
PSEAE_PA1727	VRAQDTIARLGGDEFV	(Kulesekara et al, 2006)
PSEAE_PA2870	LREVDLLGRLGGEEFA	(Kulesekara et al, 2006)
PSEAE_PA3343	RRPLDMAVRLGGEEFA	(Kulesekara et al, 2006)
PSEAE_WspR	SRSSDLAARYGGEEFA	(Hickman et al, 2005)
PSEPA_PA0847	LRQPDKAYRLGGDEFA	(Kulesekara et al, 2006)
RHOSP_Rsp3513	LGPADALGRIGGEEFA	(Ryjenkov et al, 2005)
SALTY_AdrA	LRGSDIIGRFGGDEFA	(Simm et al, 2005)
SYNY3_Slr1143	LRSYDILGRWGGDEFM	(Ryjenkov et al, 2005)
THEMA_TM1163	VRESDLVFRYGGDEFL	(Ryjenkov et al, 2005)
VIBCH_VCA096	CRDGVTAYRYGGEEFA	(Ryjenkov et al, 2005)
YERPS_HmsT	VRSRDIVVRYGGEEFL	(Simm et al, 2005)
Consensus	r d R GG#EF	

Allosteric Control of Cyclic di-GMP Signaling

Beat Christen, Matthias Christen, Ralf Paul, Franziska Schmid, Marc Folcher, Paul Jenoe, Markus Meuwly and Urs Jenal

J. Biol. Chem. 2006, 281:32015-32024.
doi: 10.1074/jbc.M603589200 originally published online August 21, 2006
